

## 3.5 Baryon Form Factors

### 3.5.1 Introduction

The internal structure of the nucleon is a defining problem for nuclear physics. The most basic observables which reflect the composite nature of the nucleon are its electromagnetic form factors. Indeed, historically the first direct indication that the nucleon is not elementary came from measurements of the form factors in elastic electron–proton scattering [164]. The elastic electric and magnetic form factors characterize the distributions of charge and magnetization in the nucleon as a function of spatial resolving power. Further, the elastic and transition form factors can be described and related to other observables through the use of generalized parton distributions. Therefore, this topic connects strongly to other thrusts of the 12 GeV program.

### 3.5.2 Context and Motivation

The nucleon elastic form factors are defined through matrix elements of the electromagnetic current,  $J_\mu = \bar{\psi}\gamma_\mu\psi$ , as:

$$\langle N(P')|J_\mu(0)|N(P)\rangle = \bar{u}(P') \left( \gamma_\mu F_1(Q^2) + \frac{i\sigma_{\mu\nu}q^\nu}{2M} F_2(Q^2) \right) u(P), \quad (3.52)$$

where  $P$  and  $P'$  are the initial and final nucleon momenta, and  $q = P - P'$  is the momentum transferred to the nucleon, with  $Q^2 = -q^2$ . The Sachs electric and magnetic form factors are defined in terms of  $F_1$  and  $F_2$  as:

$$G_E(Q^2) = F_1(Q^2) - (Q^2/4M^2) F_2(Q^2), \quad (3.53)$$

$$G_M(Q^2) = F_1(Q^2) + F_2(Q^2). \quad (3.54)$$

Electromagnetic transition form factors may be similarly defined. In this case the final state is no longer a nucleon but rather may be a resonance state:  $\langle R(P')|J_\mu(0)|N(P)\rangle$ .

The elastic form factors at low  $Q^2$  are known to approximately follow a dipole form,  $G_D(Q^2) \propto 1/(1 + Q^2/Q_0^2)^2$ , with  $Q_0^2 \approx 0.71 \text{ GeV}^2$ . This behavior can be qualitatively understood within a vector meson dominance picture, in which the virtual photon interacts with the nucleon after fluctuation into a virtual vector meson. However, deviations from the dipole form have been observed, and it is important to understand the nature of the deviations, particularly at larger  $Q^2$ .

At the other extreme of asymptotically large  $Q^2$ , the elastic form factors can be described in terms of perturbative QCD [165]. Here the short wavelength of the highly virtual photon enables the quark substructure of the nucleon to be cleanly resolved. Just where the perturbative behavior sets in is still an open question, however, which must be resolved experimentally. Evidence from recent experiments at Jefferson Lab and elsewhere suggests that non-perturbative effects still dominate the form factors

at least for  $Q^2 < 10 \text{ GeV}^2$ . For example, the  $Q^2$  dependence of the  $G_E$  and  $G_M$  form factors, which is expected to be the same in perturbative QCD, is observed to be rather strong in the  $G_E/G_M$  ratio for the proton out to  $Q^2 \approx 5 \text{ GeV}^2$  [166].

Theoretical guidance on the form factors in the transition region can be obtained from lattice QCD. It may be anticipated that these calculations will have achieved a degree of accuracy that easily surpasses that currently available for the neutron at high  $Q^2$  by the time CLAS<sup>++</sup> is taking data [167]. Challenging these fundamental calculations with high-precision data for both the proton and the neutron out to high  $Q^2$  will provide an important test of their accuracy.

Understanding the transition from the low to high  $Q^2$  regions is vital not only for determining the onset of perturbative behavior. Form factors in the transition region are very sensitive to mechanisms of spin-flavor symmetry breaking, which cannot be described *in principle* within perturbation theory. A classic example is the electric form factor of the neutron,  $G_E^n$  [168], which is identically zero in a simple valence quark picture, and whose non-zero value can only be understood in terms of non-perturbative mechanisms, such as the hyperfine interaction between quarks [169], or a pion cloud [170].

The  $Q^2$  dependence of the elastic electric and magnetic form factors of the nucleon reflects the dynamics of the quark constituent degrees of freedom in a region where confinement plays an important role. Because the electromagnetic current couples to the charged quark constituents, one can decompose the form factors into a sum over the various quark contributions:

$$G_{E,M}(Q^2) = \sum_{q=u,d,\dots} e_q G_{E,M}^{(q)}(Q^2) . \quad (3.55)$$

To determine the contribution  $G_{E,M}^{(q)}$  from each individual quark flavor requires measurement of the form factors of both the proton and neutron. However, at present, precision data at high  $Q^2$  exist only for the proton, as may be seen in Fig. 3.59.

There are other reasons why the study of form factors is of fundamental importance. They contain information on nucleon structure complementary to that which is measured through other processes, such as inclusive scattering. Recent work on generalized parton distributions has provided a unifying framework within which both form factors and structure functions can be simultaneously embedded [172, 173]. For example, the generalized parton distribution,  $H(x, \xi, t)$ , where  $t = (P - P')^2$  and  $\xi = n \cdot (P' - P)/M$  with  $n$  a light-like vector that corresponds to the matrix element of the Dirac vector current, connects the Dirac form factor  $F_1$  with the unpolarized quark distribution function,  $q(x)$ , by [172]:

$$\int_{-1}^1 dx H(x, \xi, t) = F_1(t) , \quad (3.56)$$

$$H(x, 0, 0) = q(x) . \quad (3.57)$$

The generalized parton distributions can be measured in processes such as deeply-virtual Compton scattering, or deeply-virtual meson production, at large photon vir-

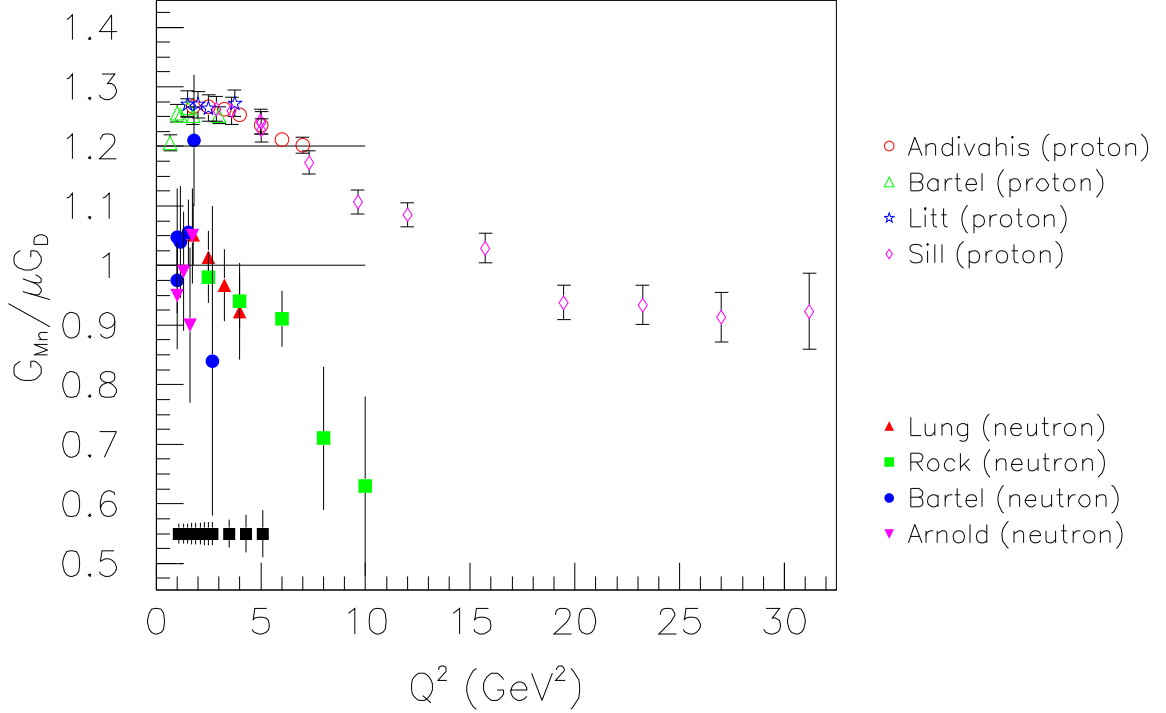


Figure 3.59: The normalized elastic proton and neutron magnetic form factors ( $G_{Mn}/G_D\mu_n$ ,  $G_{Mp}/G_D\mu_p$ ) out to high  $Q^2$ . The proton data has been shifted upward by 0.2 for clarity. Note the lack of high-quality data for the neutron at large  $Q^2$ . For more information on the referenced data, see [171]. The points plotted at 0.55 indicate the size of the anticipated errors from the CLAS E5 measurement.

tuality  $Q^2$  and small  $t$ , where one expects the process to be dominated by single quark scattering (note that here  $t$  corresponds to the square of the momentum transfer to the hadron, while  $Q^2$  is the virtuality of the photon).

Of course it is not a priori clear at which  $Q^2$  single quark scattering will dominate, so it is important to take measurements over a range of  $Q^2$ . This will also enable one to smoothly match on to the case of real Compton scattering at  $Q^2 = 0$ .

The elastic and transition form factors can be related to each other in dynamical quark models of the nucleon, and more rigorously, in the limit of QCD with a large number of colors. Therefore, within this framework, they measure different combinations of the same set of generalized parton distributions. The variety of form factor measurements accessible in CLAS<sup>++</sup> are therefore interrelated and can be interpreted within a unified analysis. Such an analysis will be very important for obtaining reliable information on these fundamental distributions.

From another perspective, the interplay between form factors and structure functions is central to the phenomenon of quark-hadron duality [61, 174, 175, 176, 177], and the transition from quark to hadron degrees of freedom in QCD. Form factors obtained in exclusive reactions can be related through local quark-hadron duality to

deep-inelastic structure functions measured in inclusive processes. For elastic scattering, the form factors can be used to predict the behavior of structure functions in the limit  $x \rightarrow 1$  [61, 178, 179, 180], which is a region very difficult to access experimentally. For the  $F_1$  structure function of the nucleon, for instance, one has at large  $Q^2$  [61, 180]:

$$F_1(x \rightarrow 1, Q^2) \propto \frac{dG_M^2(Q^2)}{dQ^2} . \quad (3.58)$$

Conversely, from data on structure functions at very large  $x$  one can extract the elastic form factors as a function of  $Q^2$  and compare with the directly measured values [174, 175].

One can similarly use quark-hadron duality to study not just the elastic case, but the entire spectrum of excited final states, and more generally the transition from resonance production to scaling in deep-inelastic scattering [181]. The form factors which parameterize transitions from the ground state to the excited states, such as  $N \rightarrow \Delta$  or  $N \rightarrow S_{11}$ , contain rich information about the spatial distribution of quarks inside the nucleon.

The  $N \rightarrow \Delta$  transition form factor is particularly important given the prominent role that the  $\Delta$  is known to play in hadron structure [170]. The previously observed  $Q^2$  dependence of the  $\gamma^* N \Delta$  form factor is qualitatively different from the  $Q^2$  dependence of the form factors of the other resonances [182]. Moreover, the contribution of the  $N \rightarrow \Delta$  transition to the polarization asymmetry

$$A_1 = \frac{\sigma_{1/2} - \sigma_{3/2}}{\sigma_{1/2} + \sigma_{3/2}} , \quad (3.59)$$

where  $\sigma_{1/2(3/2)}$  is the virtual photoabsorption cross section for total  $\gamma^*$ -nucleon spin projection  $1/2$  ( $3/2$ ), is known to be large and negative at low  $Q^2$ , while the same asymmetry at large  $Q^2$  is positive. Understanding this transition, and the related non-trivial  $Q^2$  dependence of the Gerasimov-Drell-Hearn sum rule at intermediate  $Q^2$ , requires a precise determination of the  $\gamma^* N \Delta$  form factor over a large range of  $Q^2$  [183].

The next lowest excited state after the  $\Delta$  is the negative parity partner of the nucleon, the  $S_{11}$  resonance. In the limit of exact chiral symmetry, the masses of the nucleon and its parity partner would be degenerate, so that the properties of the  $S_{11}$  form factor reveal fundamental aspects of dynamical chiral symmetry breaking in QCD.

### 3.5.3 Form Factor Measurements

There are several examples of form factors which should be accessible with CLAS<sup>++</sup>.

## Nucleon Elastic Form Factors

The form factor accessible in CLAS<sup>++</sup> that reaches the highest  $Q^2$  is the neutron magnetic form factor,  $G_{Mn}(Q^2)$ . This is obtained by an extension of the method used in Jefferson Lab experiment E94-017[33]. In this method, an unpolarized cryogenic liquid deuterium target is employed as a 'neutron target,' and the ratio of e-n events to e-p events off deuterium is measured. The proton is detected in the drift chambers and identified by time-of-flight, while the neutron is detected in the forward calorimeters with high efficiency. A cut on  $W$  selects quasi-elastic kinematics for the neutron and the proton. In the conceptual limit where the neutron and proton are considered as free in the deuteron, the e-n/e-p ratio can be directly related to the free form factors of the proton and neutron. Using the more accurately determined proton form factors and an estimate of the neutron electric form factor, one derives the magnetic form factor from the deuteron quasi-elastic cross section.

There are a number of factors which affect the accuracy of the measured  $G_{Mn}$ . While these are the same for low and high  $Q^2$ , their relative importances change. As long as  $G_{Mn}$  is much larger than  $G_{En}$ , uncertainty of the latter does not contribute significantly to the uncertainty in  $G_{Mn}$ . The proton magnetic form factor must also be quite well-known, and the proton's electric form factor must be reasonably well-determined. In quasi-elastic kinematics, corrections to the ratio due to the binding of the nucleons within the deuteron are expected to become increasingly smaller at high  $Q^2$ , and work is in progress to quantify these corrections within a reliable relativistic theory. The solid angles within which the proton and neutron are measured must be known to be equal; this problem is not expected to be very different at high momentum transfer, since these are essentially geometric issues.

The neutron detection efficiency, which must be known accurately in this method, will be more stable at high  $Q^2$ . This is because the intrinsic detection efficiency in the electromagnetic shower calorimeter plateaus to a nearly constant value for neutron momenta above approximately 1.75 GeV/c. The detection efficiency was continuously monitored in experiment E94-017 using a novel dual-cell target which allowed two target cells to be simultaneously in the beam. The upstream target contained cryogenic liquid deuterium, while the downstream target contained cryogenic liquid hydrogen. The neutron detection efficiency was thereby continuously measured using the exclusive reaction  $p(e, e'\pi^+)n$  from the proton target.

There are two factors which are expected to become much more important at high  $Q^2$ ; both essentially have to do with isolating the reaction of interest. The first is that the quasi-elastic scattering rate becomes small relative to inelastic processes nearby in the  $W$  spectrum. The tails of these processes therefore become an important contamination underneath the region of quasi-elastic scattering. The second effect is the kinematic broadening of the  $W$  peak. These two effects, taken together, mean that there may not even be a visible enhancement in the  $W$  spectrum due to this process for  $Q^2 > 8 \text{ GeV}^2$ , independent of experimental resolution. Previous measurements of  $G_{Mn}$  at high  $Q^2$ , using inclusive electron scattering, encountered this limitation[184].

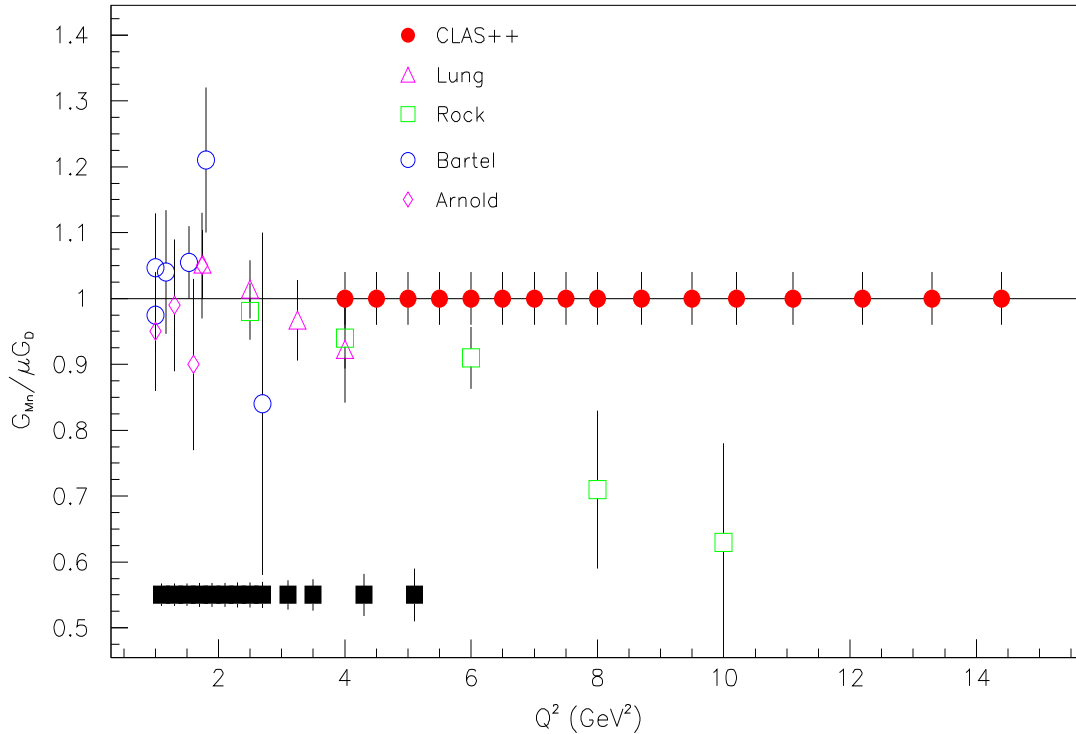


Figure 3.60: Predicted neutron form factor data obtained from CLAS $^{++}$  for a running period of 45 days. For more information on the referenced data, see [171]. The points plotted at 0.55 indicate the size of the anticipated errors from the CLAS E5 measurement.

These difficulties can be overcome in CLAS $^{++}$  using two types of cuts that do not introduce bias into the ratio measurement. First, the angle between the virtual photon and the detected nucleon is very small for quasi-elastic kinematics. Eliminating angles that are not consistent with the quasi-elastic process removes much of the inelastic background. Second, the hermiticity of CLAS $^{++}$ , and its increased capability for detection of neutrals, means that events with in-time charged particles that are inconsistent with quasi-elastic scattering can be vetoed with high efficiency, as can neutral hit pairs reconstructing to the  $\pi^0$  mass. In this way, the events of interest can be separated from inelastic events.

The expected quality of the measurement feasible is seen in Fig. 3.60. The errors are dominated by systematic errors even at the highest  $Q^2$  as a result of the increased luminosity limit from the upgraded detectors. It is clear from this figure that a substantial improvement of our understanding of the neutron elastic magnetic form factor will result from the upgrade to CLAS $^{++}$ .

## Electromagnetic Transition Form Factors

The excitation of nucleon resonances is a prominent feature of strong interaction physics in the non-perturbative domain. CLAS measurements carried out to date on

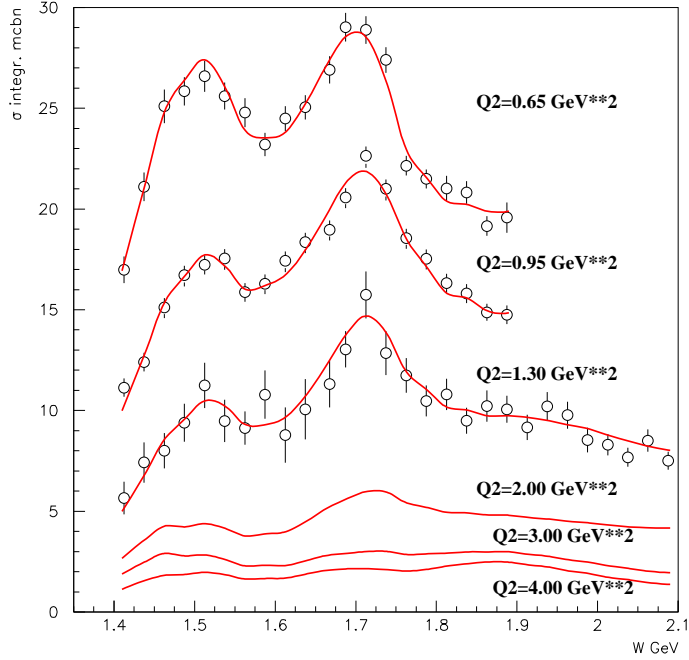


Figure 3.61: Preliminary CLAS data for  $\gamma^*p \rightarrow \pi^+\pi^-p$  [185], [186] compared to model calculations [187][188]. The photocouplings for all states and the strong couplings for  $P_{13}(1720)$ ,  $D_{13}(1700)$  are from a fit to CLAS data, while the strong decays of other states are estimated based on the analysis of [189][190] as described in [187]. The curves for  $Q^2 > 1.5 \text{ GeV}^2$  are model predictions [187][188] (see text).

excited nucleons in a variety of exclusive channels have yielded precise information on both the dominant and the weakly excited multipoles of the  $P_{33}(1232)$  resonance in single pion production [191] and for the  $S_{11}(1535)$  excitation in eta production [192]. First data on  $N^*$  electromagnetic form factors for many states with masses above 1.6 GeV have been obtained in studies of exclusive  $\pi^+\pi^-$  production on the proton at  $W < 2.1 \text{ GeV}$  and  $Q^2 < 1.5 \text{ GeV}^2$  [185][186][193]. The analysis of electromagnetic form factors for nucleon excitations  $< 2.1 \text{ GeV}$  in the  $\pi^+\pi^-$  channel [193], performed within the framework of the Single Quark Transition Model (SQTm) [194] has demonstrated that the data can be described (Fig. 3.61) with  $N^*$  photocouplings consistent to within 30% of the SQTm predictions. This supports the picture that a single quark transition between coherent three-quark configurations in the ground and excited nucleon states is an important mechanism for exciting nucleon resonances for  $Q^2 < 1.5 \text{ GeV}^2$ . CLAS<sup>++</sup> will offer the opportunity to study the evolution of the  $N^*$  excitation mechanism from coherent interactions with constituent quarks to hard interactions with a single quark for small distances with  $Q^2$  of the order of  $10 \text{ GeV}^2$ .

At this transition scale we could perhaps gain access to the quark momentum distribution for excited nucleon states. A phenomenological analysis [187][188] may be adequate to analyze the data, and one could hope to observe manifestations of sea quark contributions to  $N^*$  structure as suggested in [195].

Among the electromagnetic transition form factors accessible to CLAS<sup>++</sup>, those for the  $S_{11}(1535)$  and  $\Delta(1232)$  are particularly noteworthy. Because the  $S_{11}$  resonance has a large branching ratio to  $(N, \eta)$ , the resonance transition form factor for the  $N \rightarrow S_{11}(1535)$  transition offers a unique signature which is likely to provide substantial immunity to background resonances and non-resonant backgrounds. The  $\eta$  meson may be detected through the missing mass technique and also may be detected directly, taking advantage of the enhanced hermiticity and photon reconstruction capability of CLAS<sup>++</sup>. The prospect of having an overdetermined final state with a substantial acceptance means that a very high quality analysis will be feasible. A clean measurement will be relatively straightforward to obtain.

The  $\Delta(1232)$  resonance should also present a favorable opportunity for study out to higher  $Q^2$ . Because the resonance is well-isolated, backgrounds will be suppressed, and an adequate count rate will be obtained. As in the previous reaction, overdetermined final states in both the  $\pi^+$  and  $\pi^0$  channels should be accessible with relatively high acceptance, ensuring the reliability and completeness of the analysis. This should also help to identify the fraction of non-resonant background, which may be the primary experimental challenge. Improved angular resolution and coverage of the angle  $\phi_\pi^*$  between the hadronic and lepton scattering planes will permit CLAS<sup>++</sup> to push the separation of  $\sigma_{TT}$  and  $\sigma_{LT}$  into unexplored regions of  $Q^2$ . These structure functions measure the interference between helicity-conserving and non-conserving amplitudes and should vanish in the pQCD limit. Current CLAS data show no evidence of a trend toward this limit in  $\sigma_{TT}/\sigma_{TOT}$  in the region of the  $\Delta(1232)$ , although above and below the  $\Delta$  a rapid decrease in helicity non-conservation is evident (Fig. 3.62). Furthermore, a multipole analysis of  $\sigma_{LT}$  of data from CLAS and Hall C indicate an *increase* in the ratio of the longitudinal-scalar coupling  $S_{1+}$  to the magnetic dipole  $M_{1+}$  as  $Q^2$  increases, while pQCD strictly requires  $S_{1+}/M_{1+} \rightarrow \text{constant}$ . Figure 3.63 shows projected errors of a  $S_{1+}/M_{1+}$  measurement with CLAS<sup>++</sup>.

The information on the  $N^*$  excitation amplitude is very important in studies of quark-hadron duality as suggested in [196][197]. The approach taken by [187][188] allows extraction of the resonant amplitude averaged over resonant state widths.

A prominent feature of the double charged pion production cross-section is a pronounced resonant structure at  $W = 1.7$  GeV (Fig. 3.61) observed for the first time by CLAS. This structure was not seen in previous experiments with real photons [198], nor with hadron probes [189][190]. It was found [185] that this structure could be described in two ways: a) by assuming strong couplings of  $N^*$  from recent published analyses [189][190], a new missing baryon state could be implemented with the quantum numbers  $P_{13}(1720)$ , determined from fitting the data; b) by using known states with drastically modified strong couplings that are significantly different from recent